TITLE: BTK inhibitors synergize with 5-FU to treat drug-resistant TP53-null colon cancers

AUTHORS: Marialuisa Lavitrano[1*], Leonarda Ianzano[1], Sara Bonomo[1], Annamaria Cialdella[1], Maria Grazia Cerrito[1], Fabio Pisano[1], Carola Missaglia[1], Roberto Giovannoni[1§], Gabriele Romano[1#], Chelsea M. McLean[2], Emile E. Voest[2], Filomena D'Amato[3], Barbara Noli[3], Gian Luca Ferri[3], Marco Agostini[4.5], Salvatore Pucciarelli[4], Kristian Helin[6], Biagio Eugenio Leone[1], Vincenzo Canzonieri[7] and Emanuela Grassilli[1*]

AFFILIATIONS:

[1]School of Medicine and Surgery, University of Milano-Bicocca, Monza, Italy.

[2]Department of Molecular Oncology and Immunology, The Netherlands Cancer Institute, Amsterdam, The Netherlands.

[3]NEF-Laboratory, Department of Biomedical Science, University of Cagliari, Cagliari, Italy.

[4]First Surgical Clinic Section, Department of Surgery, Oncology and Gastroenterology, University of Padova, Padova, Italy.

[5]Department of Nanomedicine, The Methodist Hospital Research Institute, Houston, Texas, USA.

[6]Center for Epigenetics, Sloan Kettering Institute, Memorial Sloan Kettering Cancer Center, New York, New York, USA.

[7]Pathology Unit and CRO Biobank, CRO Aviano National Cancer Institute, Aviano, Pordenone, Italy.

[*] **Correspondence to:** Marialuisa Lavitrano, PhD, Dept. of Medicine and Surgery, University of Milano-Bicocca, via Cadore, 48 - 20900, Monza (MB), Italy. Phone: +39 02 6448.8336. E-mail: marialuisa.lavitrano@unimib.it

Or Emanuela Grassilli, PhD, Dept. of Medicine and Surgery, University of Milano-Bicocca, via Cadore, 48 - 20900, Monza (MB), Italy. Phone: +39 02 6448.8050. E-mail emanuela.grassilli@unimib.it,

§ Roberto Giovannoni current address: University of Pisa, Department of Biology, Pisa, Italy

Gabriele Romano current address: Department of Translational Molecular Pathology, University of Texas MD Anderson Cancer Center, Houston, TX, USA

Running title: p65BTK targeting in TP53-null drug-resistant colon cancers No conflicts of interest were declared.

Abstract

Colorectal cancer is the fourth cause of death from cancer worldwide mainly due to the high incidence of drug-resistance. During a screen for new actionable targets in drugresistant tumours we recently identified p65BTK - a novel oncogenic isoform of Bruton's tyrosine kinase. Studying three different cohorts of patients here we show that p65BTK expression correlates with histotype and cancer progression. Using drug-resistant TP53-null colon cancer cells as a model we demonstrated that p65BTK silencing or chemical inhibition overcame the 5-fluorouracil resistance of CRC cell lines and patientderived organoids and significantly reduced the growth of xenografted tumours. Mechanistically, we show that blocking p65BTK in drug-resistant cells abolished a 5-FUelicited TGFB1 protective response and triggered E2F-dependent apoptosis. Taken together, our data demonstrated that targeting p65BTK restores the apoptotic response to chemotherapy of drug-resistant CRCs and gives a proof-of-concept for suggesting the use of BTK inhibitors in combination with 5-FU as a novel therapeutic approach in CRC patients.

Keywords: Colon cancer; p65BTK; BTK inhibitors; drug-resistance; TP53

Introduction

Colorectal cancer (CRC) is the fourth leading cause of death from cancer worldwide [1]. The standard therapeutic approach is represented by surgery combined with radiotherapy and/or chemotherapy, depending on tumour site and progression of disease [2–4]. 5-fluorouracil (5-FU) is the main chemotherapeutic agent for advanced CRC and — when used in combination (doublet or triplet plus bevacizumab or antiEGFR) – initial responses are up to 55–65% [5–8]. However, despite significant progress regarding early detection and treatment of colorectal cancer, a high proportion of patients rapidly become drug-resistant and eventually succumb to metastatic disease [9]. A main cause of drug-resistance is the loss/ inactivation of the *TP53* tumour suppressor gene [10], occurring in the vast majority of advanced stage CRCs [11]. Identification of new therapeutic approaches to target 5-FU-resistant CRC is of utmost importance to obtain further improvements in advanced CRC survival.

Bruton's tyrosine kinase (BTK) is 77 kDa non-receptor tyrosine kinase playing a pivotal role in B-cell physiology where it transduces activation, proliferation, maturation, differentiation and survival signals [12]. Due to its hyper-activation in autoimmune disease and over-expression in some B-cell neoplasia, BTK emerged as a molecular target [13] leading to the approval of ibrutinib - the first specific inhibitor - for the treatment of certain types of B-cell malignancies [14]. In recent years, expression of BTK or of an 80 kDa isoform has been reported in solid tumours such as neuroblastoma, glioblastoma, oesophageal, breast and prostate cancers where its inhibition reduces cell viability [15–19].

We found *BTK* in a screen aimed at identifying kinases whose activation sustains resistance to 5-FU in CRC cells lacking TP53 [20] and identified p65BTK as a novel isoform expressed in CRC [21]. We demonstrated that only the *p65BTK*-encoding, but not *p77BTK*-encoding mRNA, is expressed in colonic tissue where, accordingly, only the p65BTK protein

is present [21]. Successively, we found p65BTK expression also in glioblastoma [22] and NSCLC [23]. *p65BTK* mRNA is transcribed from a different promoter, contains a different first exon and its translation produces a protein lacking the first 86 N-terminal amino acids, corresponding to the majority of the Pleckstrin Homology domain. Notably, structural studies indicated that the lack of the N-terminal leads to increased levels of spontaneous p65BTK activation [24]. Despite that *p65BTK*encoding mRNA is expressed at very low levels, the protein is very abundant due to RAS/MAPK pathway-mediated translational regulation [21, 23]. In addition, p65BTK is a potent oncogene product acting downstream of RAS and an obligate effector of RASmediated transformation, and its targeting by BTK inhibitors has an anti-proliferative effect on CRC cell lines [21].

Here we show that the vast majority of CRC patients express medium to high p65BTK levels that significantly increase with the grade of CRC, and that BTK inhibitors sensitize drug-resistant TP53-null colon cancer cell lines, patient-derived organoids and xenografts to 5-FU. Mechanistically, we prove that inhibiting p65BTK in the presence of 5-FU blunts 5-FU-induced TGFB1-mediated transcription and induces E2F-mediated transcription. As a consequence, a 5-FU-elicited TGFB1 protective response is abolished and E2F-dependent apoptosis is triggered. Taken together, these results reveal a role for p65BTK in sustaining drug-resistance in TP53-null CRCs and suggest that administration of BTK inhibitors in combination with 5-FU in CRC patients is worthy of consideration

Methods

Details of reagents, Taqman primers, cell culture protocols, antibody information and the ELISA protocol are provided in Supplementary material, supplementary Materials and methods.

Cell death assays

Cells were seeded overnight in triplicate at 60–70% confluence. The following morning they were treated or not with the indicated concentrations of drugs or combination of drugs. Cell death was evaluated by Trypan blue exclusion after 72 h treatment. For *exvivo* experiments, 100 organoids/well were plated in 5 μl of Geltrex (Thermofisher, Breda, The Netherlands) in a 96-well plate, in triplicate, adding 100 μl of specific medium, with or without drug(s). At time 0 and after 72 h, viability was evaluated using the CellTiter-Glo® Luminescent Cell Viability Assay (Promega, Leiden, The Netherlands) following the manufacturer's instructions. Results were expressed as the percentage change relative to the initial cell number (T0). All cell death assays were repeated 3 times (*n*=3). The Combination Index (CI) was calculated as reported by Giordano *et al* [23]. For details see supplementary material, Supplementary materials and methods.

Luciferase reporter assays

2×10^4 cells/well were seeded in quadruplicate on Cignal™ Finder (Qiagen, Milan, Italy) 96-well plates for reverse transfection according to the manufacturer's protocol. Medium was changed after 48 h and cells treated with 200 μM 5-FU, 20 μM ibrutinib or their combination for 4, 8 and 16 h. Cells were lysed, and luciferase expression determined by Nano-Glo® Dual-Luciferase® Reporter Assay System according to the manufacturer's protocol (Promega, Milan, Italy). Reporter assays were repeated 3 times for each time point (*n*=3). Results are plotted as fold-change, calculated as the ratio: values of treated cells/values of untreated cells, and where the value of untreated cells is set at 1.

RT-qPCR assays

Total RNA was extracted using TRIzol reagent (Invitrogen, Thermofisher, Monza, Italy), followed by clean up using RNeasy Mini/Midi Kits (Qiagen, Milan, Italy). One microgram of RNA from HCT116p53KO treated with 200 μM 5-FU, 20 μM ibrutinib or their combination for different times was reverse transcribed using a RevertAid H Minus First Strand cDNA Synthesis Kit (Thermofisher) in a final volume of 20 μl. An aliquot of the resulting cDNA (1 μl) was diluted 1:100 and used for qPCR assays performed in 25 μl reactions containing 12.5 μl 2x TaqMan Master Mix (Applied Biosystems,

Thermofisher), 1 μl of TaqMan Assay (Applied Biosystems). Assays were loaded in triplicate and included in each 96-well assay plate were control qPCR reactions for *GAPDH* were used as a reference for normalisation. The default ABI StepOnePlus

System amplification conditions were used. The comparative CT method (2−ΔΔCT) method was used for expression analysis. The experiment was repeated twice (*n*=2).

Somatic mutation PCR assay

DNA was extracted from pelleted cells using the DNeasy Blood & Tissue Kit (Qiagen). The Human Colon Cancer qBiomarker Somatic Mutation PCR array (Qiagen) was used to detect the most frequent somatic mutations in human colon cancer samples. DNA samples (0.5 μg) were added to the reaction mix and to the array and the PCR cycling

conditions were set according to the manufacturer's instructions. The 2−ΔΔCT method was used for the mutation analysis as suggested by the kit instructions.

Western blotting analysis

Protein extracts were prepared using high-salt lysis buffer (HEPES 50 mM, pH 7.5, NaCl 500 mM, DTT 1 mM, EDTA 1 mM, 0.1% NP40) supplemented with 1% protease inhibitor cocktail (Sigma-Aldrich, Milan, Italy). Cell and tissues lysates (10–20 μg) were separated

on 10% NuPAGE gels (Invitrogen, Thermofisher, Monza, Italy), transferred onto a nitrocellulose membrane and incubated with antibodies according to standard protocols.

Patients

p65BTK expression levels were measured by ELISA in samples from two cohorts of patients and by immunohistochemistry (IHC) in samples from a third cohort. Samples analysed by ELISA derived from cohorts of patients with a clinical diagnosis of colon cancer, consecutively admitted to the Department of Surgery, Oncology and Gastroenterology, University of Padua (*n*=61, Tumour Biobank Program P448, Dept of Surgery, Oncology and Gastroenterology, University of Padua - Italy) and to Desio Hospital (*n*=19), respectively. All samples were classified by a pathologist by Grade (13) and by Stage (I-IV). Samples analysed by IHC were obtained from a cohort of patients (*n*=174, CRO-Biobank facility) with a clinical diagnosis of colon cancer consecutively admitted to the CRO Aviano-IRCCS, National Cancer Institute, Aviano, and classified as Stage I-III. Patient's samples were collected after informed consent in accordance with the Declaration of Helsinki and after approval by the Ethics Committee of the University of Milano-Bicocca, by the local Ethics Committee of the Integrated University Hospital Trust of Padova and by CRO Aviano's Ethics Committee and Internal Review Board.

Immunohistochemistry (IHC)

FFPE tumour samples were prepared and slides probed with anti-p65BTK BN30 polyclonal antibody according to standard IHC procedures. BN30 polyclonal antibody production and characterization was described previously [23]. Staining intensity and percentage of positive tumour cells were evaluated as absent, weak+, moderate++, or strongly positive+++; and 0: score 0; 1-25%: score 1; 26-50%: score 2; 51-75%: score 3; 76-100% score 4, respectively.

ELISA

Snap-frozen specimens were lysed in RIPA buffer and p65BTK levels were measured by a competitive ELISA, set up with the polyclonal antibody BN33 (IgG fraction), using the corresponding peptides conjugated to ovalbumin for plate coating, as well as standards. For details see supplementary material, Supplementary materials and methods.

Xenografting

All animal experiments were carried out accordingly to Directive2010/63/EU and Italian D.Lgs.116/1992 on animal use for scientific purposes and according to a protocol approved by the local ethical committee of Takis, srl, Rome, Italy (the contract research organisation where the experiments were performed). Tumours were established in CD1 nude mice as described [20]. When HCT116p53KO xenografts reached the average volume of 100 mm^3 (day 7 post-engraftment), animals were randomised (6/group) and given vehicle or ibrutinib 25 mg/kg (oral gavage, 5 days/week); 5-FU was given IP twice per week. The treatments were continued for 3 weeks, with the tumours monitored daily and measured with callipers once per week.

Statistical analysis

For *in vitro* and *ex vivo* experiments, results were analysed using two-tailed Student's *t*tests. For *In vivo* experiments, statistical significance was determined using a Kruskal– Wallis non-parametric test (normal distribution not assumable), followed by a Nemenyi– Damico– Wolfe–Dunn test for multiple pairwise comparisons between groups. In all cases, a P value <0.05 was considered as significant.

Results p65BTK expression correlates with histotype and cancer progression.

188 To assess the expression of p65BTK in tumour tissues, we developed and validated
189 specific polyclonal antibodies for this isoform that did not cross-react with p77BTK
190 (supplementary material, Figure S1) [23]. We quantified p65BTK expression in three
191 different cohorts of colon cancer patients: samples from two cohorts of 19 and 61 CRC
192 patients were analysed by ELISA and those from a third cohort of 174 CRC patients were
193 analysed by IHC performed on FFPE sections. Interestingly, ELISA analysis of
194 normal/tumour sample pairs showed that p65BTK expression levels significantly increased
195 with histological tumour grade (Figure 1A), suggesting an inverse correlation between
196 p65BTK expression levels and cellular differentiation. Accordingly, we found p65BTK
197 expressed also in FACS-purified CD133+ colon cancer stem cells (CSC) [25] and CSC-
198 enriched organoids prepared from CRC patients' tumour tissue (Figure 1B). p65BTK
199 expression was found in adenoma and adenocarcinoma but not adenosquamous
200 carcinoma (Figure 1C).
201 A more detailed analysis of p65BTK expression was performed on a third cohort
202 using IHC, which was scored on the staining intensity (absent, weak, moderate, or strongly
203 positive) and the percentage of stained tumour cells in the sample (Figure 1D). We found a
204 medium-to-strong intensity (++/+++) of p65BTK staining in 34/43 (79.1%) samples from
205 Stage I patients, in 36/44 (81.8%) samples from Stage II patients and in 57/87 (65.5%)
206 samples from Stage III patients (Figure 1E, left). In detail, only 2/43 samples (4.7%) from
207 Stage I patients did not express p65BTK, positive cells ranged from 1 to 30% in 2/43
208 samples (4.7%), from 30 to 70% in 13/43 samples (30.2%) whereas in the remaining 26/43
209 samples (60.5%) the percentage of cell expressing p65BTK ranged from 71 to 100%. Only
210 1/44 sample (2.3%) from Stage II patients was p65BTK-negative; 7/44 (15.9%) showed 1–
211 30% p65BTK-stained cells, 6/44 (13.6%) had 31–70% positive cells and in the remaining
212 30/44 samples (68.2%) 71–100% cells expressed p65BTK. 8/87 samples (9.2%) from
213 Stage III patients did not express p65BTK, in 12/87 samples (13.8%) the percentage of

p65BTK-stained cell ranged from 1–30%, in 20/87 samples (23%) p65BTK-expressing cells were 30–70% and positivity was between 71 and 100% cells in the remaining 47/87 samples (54%) (Figure 1E, right).

Notably, p65BTK expression was found as early as at the adenoma stage. Therefore, based on its widespread and early expression, p65BTK might be causally involved in CRC development even though further studies are needed to assess this potential role.

p65BTK expression levels determine 5-FU sensitivity of colon carcinoma cells and its silencing/inhibition abolishes 5-FU resistance of TP53-null colon carcinoma cells.

Previously, we have shown that p65BTK inhibition affects the growth and survival of colon cancer cells [21]. Therefore, we sought to determine the effect of p65BTK inhibition on the response of drug-resistant colon cancer cells to 5-FU, using the well characterised model of drug-resistance represented by HCT116p53KO cells treated with 200 μM 5-FU [26]. This experimental model is representative of the single bolus schedule of patient treatment where after a single injection of 5-FU, plasma concentration of the drug is of 27.4 ng/ml (=170 μM) at 24 h [27]. Either stable (Figure 2A) or transient (Figure 2C) reduction of p65BTK rendered drug-resistant HCT116p53KO cells sensitive to 5-FU to the same extent as parental drug-sensitive HCT116 cells (Figure 2B,D). Conversely, over-expression of p65BTK, but not its kinasedead counterpart, protected drug-sensitive HCT116 cells from 5-FU-induced cell death (Figure 2E,F). These results indicate that p65BTK kinase activity is essential for protecting from cytotoxicity triggered by 5-FU. Notably, p65BTK levels seem to be critical for sensitivity to 5-FU: in fact, co-treating HCT116 sensitive cells with non-toxic concentrations of ibrutinib (20 μM) and 5-FU (10 μM) resulted in massive cytotoxicity,

237 comparable to that obtained when using maximally cytotoxic concentrations of 5-FU alone
238 (Figure 2G). Conversely, a dose-dependent re-sensitization to 5-FU of drugresistant
239 HCT116p53KO cells occurred in presence of increasing concentrations of ibrutinib (Figure
240 2H). We previously demonstrated that p65BTK levels are posttranscriptionally regulated
241 downstream of RAS [21]. We confirmed this finding by showing that *p65BTK* mRNA
242 expression levels were the same in all cell lines tested, (supplementary material, Figure S2,
243 panel A) - independently of the genetic background - whereas the protein levels were higher
244 in cells bearing a mutation in the RAS/MAPK pathway (supplementary material, Figure S2,
245 panel B). Accordingly, the combination ibrutinib + 5-FU was significantly more effective in
246 drug-resistant HCT116p53KO cells (*RAS* mt) versus Caco-2 cells (*TP53* mt/*RAS* wt)
247 (supplementary material, Figure S3).

248 We confirmed the role of p65BTK in sustaining drug-resistance by demonstrating that
249 the addition of non-toxic concentrations of different BTK inhibitors (ibrutinib, AVL292,
250 RN486, CGI1746, ONO-4059) to 5-FU allowed representative [28], drug-resistant TP53-null
251 colon cancer cell lines with different genetic backgrounds (supplementary material, Table
252 S1) to undergo cell death upon 5-FU treatment (Figure 3). Notably, the combination
253 between any given BTK inhibitor and 5-FU resulted in a strong synergistic effect (Table 1).
254 We tested a range of ibrutinib concentrations (up to 20 μM) already reported in the literature
255 for treating B cell lines, leukemic primary cells, and some solid tumours [16, 19, 29–33].
256 Recently, it has been shown that besides inhibiting BTK, ibrutinib is also a potent EGFR
257 inhibitor [34–36]. Therefore, to verify that re-sensitisation to 5-FU upon ibrutinib treatment
258 is via p65BTK, and not EGFR inhibition, we compared levels of cytotoxicity induced by 5-
259 FU in TP53-null drug-resistant colon cancer cells in combination with ibrutinib or with two
260 second-generation EGFR inhibitors, afatinib and poziotinib [37]. After determining the
261 optimal doses of the inhibitors required to completely suppress EGFR phosphorylation, we
262 tested their effect on cell viability when used in combination with 5-FU. When added to 5-

FU at doses completely suppressing EGFR phosphorylation (supplementary material, Figure S4 A,B), only ibrutinib induced significant cell death of drug-resistant cells, whereas addition of either afatinib or poziotinib did not modify the response of TP53-null colon carcinoma cells to 5-FU (supplementary material, Figure S4C). Moreover, adding ibrutinib to EGFR inhibitors resulted in a synergic effect (supplementary material, Figure S4D), further excluding that the action of ibrutinib might be due to its binding to EGFR.

Next, we determined that the type of cell death induced by 5-FU upon p65BTK inhibition was apoptosis, as demonstrated by induction of caspase-3/-7 activity (supplementary material, Figure S5A) and by the protection from cytotoxicity observed upon addition of the pan-caspase inhibitor Q-VD-OPh to the combination 5-FU + ibrutinib (supplementary material, Figure S5B). Finally, we showed that p65BTK inhibition restored the apoptotic response to 5-FU via unbalancing the anti-/proapoptotic ratio of BCL2-family members (supplementary material, Figure S5C). Taken together, these data indicate that p65BTK inhibition restores the apoptotic response of drug-resistant TP53-null colon carcinomas to 5-FU.

p65BTK inhibition restores the apoptotic response to 5-FU via blunting protective 5-FU-elicited TGFB1 activation and inducing pro-apoptotic E2F activation.

To explore potential cytotoxicity mechanisms elicited by 5-FU when p65BTK activity is inhibited and to obtain insight into the signalling pathways and the transcriptional programs potentially affected we measured ten cancer-related signalling pathways by reporter assays finding that only two were greatly modulated (Figure 4A,C and supplementary material, Figure S6). Interestingly, both 5-FU and ibrutinib strongly induced TGFB1 activation, which was abolished by their combination (Figure 4A). Consistent with this, TGFB1 protein levels increased upon 5-FU treatment (Figures S7A) and co-treatment with 5-FU+ibrutinib down-regulated the expression of TGFB1 targets induced by 5-FU (supplementary material, Figure S7B). Accordingly, the addition of conditioned medium

289 from 5-FU-treated drug-resistant HCT116p53KO cells reduced the apoptotic effect of 5-
290 FU+ibrutinib co-treatment whereas concomitant blockade of TGFB1 signalling restored
291 apoptosis triggered by 5-FU+ibrutinib. Finally, direct addition of TGFB1 also significantly
292 reduced 5-FU+ibrutinib-induced apoptosis (Figure 4B). In accordance, reducing 5-FU-
293 induced TGFB1 increase attenuated the resistance of HCT116p53KO cells to 5-FU
294 (supplementary material, Figure S7C).

295 E2F activation was strongly induced 8 h after treating cells with 5-FU+ibrutinib
296 (Figure 4C), followed by increased expression of pro-apoptotic E2F targets [38]
297 (supplementary material, Figure S8). Accordingly, E2F activation was instrumental to the
298 cytotoxic effect of the 5-FU+ibrutinib since cell death was significantly reduced upon
299 depletion of TFDP1, the obligate partner of E2F transcription factors [39, 40] (Figure 4D).
300 However, only when the 5-FU+ibrutinib co-treatment was performed on TFDP1depleted
301 cells in the presence of TGFB1 the percentage of cell death was reduced to the same basal
302 levels induced by 5-FU (Figure 4E). Overall, these findings demonstrate that p65BTK
303 inhibition restores 5-FU-induced cytotoxicity via concomitantly blunting a protective 5-FU-
304 elicited TGFB1 activation and inducing pro-apoptotic E2F functions.

305 ***Ex vivo* p65BTK inhibition sensitises TP53-null colon organoids to 5-FU.**

306 Data obtained from cell-based assays using 2D cultures of commercially available
307 cell lines are often only partially validated *in vivo,* since these models do not capture the
308 heterogeneity of the real patient population and do not fully mimic the *in vivo* situation, where
309 cells are in a 3D environment. Recently, to overcome these limitations in the preclinical
310 validation of novel therapeutic approaches, patient-derived 3D organoids have been
311 developed [41] and shown to recapitulate patient responses in the clinic [42]. We validated
312 the effect of p65BTK inhibition on the response to 5-FU using CSC-enriched organoids from
313 5 patients, shown to express p65BTK (Figure 1B). We characterized them for the main

mutations found in CRC and performed dose-response curves for 5-FU (supplementary material, Figure S9A) finding that 5-FU was not cytotoxic for all *TP53*-mutant tumours; an exception was TUM07 which is *TP53*-wt but functionally TP53-null due to MDM2 overexpression (supplementary material, Figure S9B). TUM09, the only *TP53*-wt tumour, was instead sensitive to 5-FU. Interestingly, when performing dose-response curves with two different BTK inhibitors, ibrutinib and AVL-292, variable levels of sensitivity towards the two drugs, likely determined by individual pharmacokinetics, were observed (supplementary material, Figure S9C). However, when combining non-toxic doses of ibrutinib or AVL-292 with 5-FU in all

TP53-null organoids a significant cytotoxic response was observed with at least one (TUM07) or both (TUM01, TUM03, ITO17) drugs (Figure 5, Table 2), confirming the benefit of p65BTK targeting in drug-resistant tumours in real heterogeneous patients' population.

In vivo p65BTK inhibition sensitises drug-resistant TP53-null colon carcinomas to 5-FU.

We verified the effect of p65BTK inhibition on the in *vivo* response to 5-FU by performing xenograft experiments. We used CD-1 nude mice inoculated subcutaneously on the left flank with drug-resistant HCT116p53KO cells and on the right flank with parental, drug-sensitive HCT16 cells [20] which served as positive control for the efficacy of 5-FU. In agreement with what observed in organoids, treatment of xenograft-bearing mice with 25 mg/kg ibrutinib [43] in combination with 60 mg/kg 5-FU did not ameliorate the response of drug-sensitive HCT116 xenografts (supplementary material, Figure S10) but significantly reduced the tumour volume and concomitantly increased the doubling time of drug-resistant HCT116p53KO xenografts (Figure 6A–C). Therefore, *in vivo* results confirm *in vitro* and *ex-vivo* data and suggest that p65BTK targeting might be useful to re-sensitize TP53-null CRC to 5-FU therapy.

Discussion

Remarkably, we found that p65BTK is expressed in the vast majority of CRCs, where its expression correlated with histotype and cancer progression (Figure 1). In particular, >90% of Stage I patients' tumour samples stained positive for p65BTK indicating that its expression is an early event during the natural history of the tumour. In general, in 60% of patients' tumoural samples from all stages >70% of the cells showed a medium-to-strong intensity of p65BTK staining. Notably, we recently showed that patients with highly expressed p65BTK (IHC intensity 3 and ≥80%) have the worst prognosis in terms of disease-free survival [44]. Therefore, given its early and extensive expression, p65BTK might be a widespread actionable target. Accordingly, using ibrutinib or other commercially available BTK inhibitors, we demonstrated the benefit of p65BTK targeting for restoring the apoptotic response to 5-FU of drug-resistant, TP53-null CRC cell lines (Figures 2, 3) and patient-derived organoids (Figure 5) and for significantly reducing tumour growth after 5-FU therapy in xenografts (Figure 6). It has recently been shown that ibrutinib, beside BTK, also potently inhibits EGFR family members [34–36]. However, our results indicate that EGFR inhibition does not contribute to the resensitization to 5-FU cytotoxic action for several reasons. First, all cell lines used in our study have a mutation in the RAS/MAPK pathway (supplementary material, Table S1) and thus are resistant to the use of EGFR inhibitors [45]. In fact, cytotoxicity was not induced by blocking EGFR phosphorylation with afatinib and poziotinib either alone or in combination with 5-FU, whereas apoptosis was instead elicited when EGFR-inhibiting doses of ibrutinib were combined with 5-FU; moreover, combining ineffective concentrations of EGFR inhibitors with ibrutinib resulted in a significant cytotoxic effect (supplementary material, Figure S2) further excluding that the action of ibrutinib might be due to EGFR binding. Second, re-sensitization occurred following reduction of p65BTK levels by functional genetic approaches (shRNA/siRNA) and

conversely, protection from 5-FU-induced cytotoxicity of sensitive cells was afforded by overexpression of p65BTK, but not its kinase-dead version (Figure 2). Finally, resensitization occured using BTK inhibitors (Figure 3) with different mechanisms of action ie, irreversible binding to Cys481 (ibrutinib and AVL-292) [46], reversible binding to unphosphorylated BTK in the SH3 domain (CGI-1746) - which leads to stabilization of the protein in an inactive conformation and prevents its auto-phosphorylation [47] - and interaction with K430 (RN486) [48], a residue critical for kinase activity [49]. Notably, independent of the mechanism of action, any inhibitor in combination with 5-FU had a strong synergistic effect (Tables 1, 2).

Mechanistically, we showed that p65BTK inhibition in TP53-null cells restored 5FU sensitivity by triggering apoptosis (supplementary material, Figure S3) and that ibrutinib abolished 5-FU-induced TGFB1-mediated transcription while inducing activation of pro-apoptotic E2F (Figure 4). We showed previously that 5-FU-induced activation of the TGFB1 pathway sustained the drug-resistance of TP53-null CRC cells, which was abolished by inhibiting TGFB1RI-mediated signalling [50]. Here, we confirm that 5-FU treatment induced TGFB1 expression and its reduction or the blockade of its downstream signalling partly re-sensitized drug-resistant cells to 5-FU (supplementary material, Figure S7, Figure 4B). It has been reported that in CRC, TGFB signalling via ATM participates in the response to DNA damage [51] which critically depends on TP53 function [52], that in turn is also activated by E2F1, given that pro-apoptotic E2F1 functions are triggered by DNA damage [53]. The finding that p65BTK inhibition in absence of TP53 blunts TGFB1 activation and activates E2F (Figure 4A,C) in response to 5-FU suggests that blocking BTK activity in TP53-null cells can compensate for the dysregulated TGFB1 and E2F1 responses to DNA damage induced by 5-FU and implies p65BTK as a critical node for the outcome of cells having sustained DNA damage.

Particularly relevant are the data obtained in CSC-enriched organoids. CSCs are characterized by high levels of drug-resistance and can effectively repopulate the tumour after chemotherapy [54]: therefore, targeting CSCs is crucial for improving therapies. Organoids display all the hallmarks of the original tissue in terms of architecture, cell-type composition, and self-renewal dynamics, capture the genetic diversities of tumour tissues and show high levels of correlation with source biopsy material, indicating that they faithfully represent original tumours [55] and therefore might be a good surrogate for precision medicine based on patient stratification [56]. Remarkably, p65BTK was expressed in purified CSCs and CSC-enriched organoids (Figure 1B) and non-toxic concentrations of BTK inhibitors in combination with ineffective concentrations of 5-FU were highly synergistic (Table 2) and efficiently killed TP53-null organoids, whereas they did not further improve 5-FU toxicity in a *TP53*-wt organoid (Figure 5 and supplementary material, Figure S9). Interestingly, in contrast with CRC cell lines, in organoids a variable sensitivity to the two different BTK inhibitors, ibrutinib and AVL-292, was evident. This variability may be due to the fact that, at variance with 2D cell cultures, organoids capture the heterogeneity of the real patients' cancer cell population and mimic the 3D *in vivo* situation. In addition, variability may reflect individual differences in drug pharmacokinetics. Although nothing is known so far about AVL-292, ibrutinib is known to be metabolized by CYP3A4 and 3A5 [57], both overexpressed in a large number of CRCs [58]. In addition, inter-individual variability of CYP3A activity linked to different genetic polymorphisms has also been shown [59]. In line with this, it has been reported that in patients with high CYP3A activity ibrutinib dosage must be increased to be therapeutically effective [60]. Therefore, the fact that, depending on the organoid, different concentrations of ibrutinib were required to sensitize them to 5-FU is likely due to different levels of CYP3A expression. Accordingly, the concentrations of ibrutinib effective on CRC cells are higher than those generally used in B cells (normal and neoplastic), that do not express CYP3A [61].

Notably, ibrutinib is already therapeutically used for certain B-cell malignancies where p77BTK is overexpressed/hyperactivated [62], and others specific BTK inhibitors, such as AVL-292 and ONO-4059, are also in clinical trials for B-cell malignancies [63, 64]. In particular, ibrutinib is indicated for patients with chronic lymphocytic leukaemia/small lymphocytic lymphoma having 17p deletion that leads to TP53 loss [65, 66]. Therefore, although we previously demonstrated that p65BTK possesses peculiar features, such as post-translational regulation and oncogenicity, not shared by p77BTK [21] both isoforms seem to share common roles in sustaining viability in the absence of TP53. In addition, a general role for BTK in cell viability is evident given that its inhibition in oesophageal cancer and neuroblastoma or inhibition of another 80 kDa isoform, expressed in breast and prostate cancers, also reduced tumour cell viability [15–19]. In addition, p65BTK seems to play a general role in sustaining drug resistance, given that its inhibition not only re-sensitize drug-resistant colon cancers to 5-FU but also bypass resistance of NSCLC cells to standard of care chemotherapy and EGFR-targeted therapy [23].

In summary, we have shown that p65BTK is expressed in the vast majority of CRCs and its inhibition restores 5-FU sensitivity of TP53-null tumours in different experimental models (*in vitro*, *ex vivo, in vivo*). In particular, its inhibition restored an apoptotic response to 5-FU via blunting a protective 5-FU-elicited TGFB1-mediated response and inducing pro-apoptotic E2F activation. Our findings suggest p65BTK as an actionable target in TP53-null CRCs where its inhibition, in combination with 5-FU, may be a promising strategy to treat drug-resistant CRCs and support the use of BTK inhibitors in combination with 5-FU in CRC patients.

Acknowledgements

This work was supported by the Italian Ministry of University and Research (MIUR) PON01_02782 and Italian Ministry of Health, RF-2010-2305526 to M.L; University of

Milano-Bicocca FAR grants 2014-ATE-0374, 2015-ATE-0447, 2016-ATE-0299 to EG. The authors wish to thank Ruggero De Maria and Lucia Ricci-Vitiani for the generous gift of lysates from purified colon cancer stem cells from patients' tissue.

Statement of author contributions

ML supervised research and provided critical revision of the manuscript; LI, SB, FP, AC, MGC, CM, RG, CMcL designed and performed experiments and analysed data; EV provided organoids, designed experiments, analysed data; FD'A, BN, GLF produced and characterized antibodies; MA, SP, BEL provided clinical samples; VC provided clinical samples, acquired and analysed data; KH provided suggestions; EG conceived and supervised research, wrote the manuscript.

REFERENCES

1. Ferlay J, Soerjomataram I, Dikshit R, *et al*. Cancer incidence and mortality worldwide: Sources, methods and major patterns in GLOBOCAN. *Int J Cancer* 2012; **136:** E359–E386.
2. Yoshino T, Arnold D, Taniguchi H *et al*. Pan-Asian adapted ESMO consensus guidelines for the management of patients with metastatic colorectal cancer: a JSMO-ESMO initiative endorsed by CSCO, KACO, MOS, SSO and TOS. *Ann Oncol* 2018; **29:** 44–70.
3. Glynne-Jones R, Wyrwicz L, Tiret E *et al*. Rectal cancer: ESMO Clinical Practice Guidelines for diagnosis, treatment and follow-up. *Ann Oncol* 2018; **29** (Supplement_4)**:**iv263.
4. Benson AB, Venook AP, Al-Hawary MM, *et al*. NCCN Guidelines Insights: Colon Cancer, Version 2.2018. *J Natl Compr Canc Netw* 2018; **16:** 359–369.

5. Loupakis F, Cremolini C, Masi G, *et al*. Initial therapy with FOLFOXIRI and bevacizumab for metastatic colorectal cancer. *N Engl J Med* 2014; **371:** 1609–1618.
6. Venook AP, Niedzwiecki D, Lenz HJ, *et al*. Effect of first-line chemotherapy combined with cetuximab or bevacizumab on overall survival in patients with KRAS wild-type advanced or metastatic colorectal cancer: a randomized clinical trial. J*AMA* 2017; **317:** 2392–2401.
7. Douillard JY, Oliner KS, Siena S, *et al*. Panitumumab-FOLFOX4 treatment and RAS mutations in colorectal cancer. *N Engl J Med* 2013; **369:** 1023–1034.
8. Ciardiello F, Normanno N, Maiello E, *et al*. Clinical activity of FOLFIRI plus cetuximab according to extended gene mutation status by next-generation sequencing: findings from the CAPRI-GOIM trial. *Ann Oncol* 2014; **25:** 1756–1761.
9. Hammond WA, Swaika A, Mody K. Pharmacologic resistance in colorectal cancer: a review. *Ther Adv Med Oncol* 2016; **8:** 57–84.
10. Housman G, Byler S, Heerboth S, *et al*. Drug resistance in cancer: an overview. *Cancers* 2014; **6:** 1769–1792.
11. Baker SJ, Preisinger AC, Jessup JM, *et al*. p53 gene mutations occur in combination with 17p allelic deletions as late events in colorectal tumourigenesis. *Cancer Res* 1990; **50:** 7717–7722.
12. Mohamed AJ, Yu L, Bäckesjö CM, *et al*. Bruton's tyrosine kinase (Btk): function, regulation, and transformation with special emphasis on the PH domain. *Immunol Rev* 2009; **228:** 58–73.
13. Hendriks RW, Yuvaraj S, Kil LP. Targeting Bruton's tyrosine kinase in B cell malignancies. *Nat Rev Cancer* 2014; **14:** 219–232.
14. Roskoski R Jr. Ibrutinib inhibition of Bruton protein-tyrosine kinase (BTK) in the treatment of B cell neoplasms. *Pharmacol Res* 2016; **113:** 395–408.

15. Li T, Deng Y, Shi Y, *et al*. Bruton's tyrosine kinase potentiates ALK signaling and serves as a potential therapeutic target of neuroblastoma. *Oncogene* 2018; **37:** 6180–6194.
16. Wang J, Liu X, Hong Y, *et al.* Ibrutinib, a Bruton's tyrosine kinase inhibitor, exhibits antitumoural activity and induces autophagy in glioblastoma. *J Exp Clin Cancer Res* 2017; **36:** 96–109.
17. Chong LIY, Aronson L, Bryant H, *et al*. Mapping genetic vulnerabilities reveals BTK as a novel therapeutic target in oesophageal cancer. *Gut* 2018; **67:** 1780–1792.
18. Eifert C, Wang X, Kokabee L, *et al*. A novel isoform of the B cell tyrosine kinase BTK protects breast cancer cells from apoptosis. *Gene Chrom Cancer* 2013; **52:** 961–975.
19. Kokabee L, Wang X, Sevinsky CJ, *et al.* Bruton's tyrosine kinase is a potential therapeutic target in prostate cancer. *Cancer Biol Ther* 2015; **16:** 1604–1615.
20. Grassilli E, Narloch R, Federzoni E, *et al.* Inhibition of GSK3B bypass drug resistance of p53-null colon carcinomas by enabling necroptosis in response to chemotherapy. *Clin Cancer Res* 2013; **19:** 3820–3831.
21. Grassilli E, Pisano F, Cialdella A, *et al.* A novel oncogenic BTK isoform is overexpressed in colon cancers and required for RAS-mediated transformation. *Oncogene* 2016; **35:** 4368–4378.
22. Sala L, Cirillo G, Riva G, *et al*. Specific expression of a new Bruton Tyrosine Kinase isoform (p65BTK) in the glioblastoma gemistocytic histotype. *Front Mol Neurosci* 2019; **12:** 2. doi: 10.3389/fnmol.2019.00002. eCollection 2019.
23. Giordano F, Vaira V, Cortinovis D, *et al*. p65BTK is a novel potential actionable target in KRAS-mutated/EGFR-wild type lung adenocarcinoma. *J Exp Clin Cancer Res* 2019; **38:** 260.
24. Joseph RE, Wales TE, Fulton DB, *et al*. Achieving a graded immune response: BTK adopts a range of active/inactive conformations dictated by multiple interdomain contacts. *Structure* 2017; **25:** 1481–1494.

514 25. Ricci-Vitiani L, Lombardi DG, Pilozzi E, *et al*. Identification and expansion of human
515 colon-cancer-initiating cells. *Nature* 2007; **445:** 111–115.
516 26. Bunz F, Hwang PM, Torrance C, *et al*. Disruption of p53 in human cancer cells alters
517 the responses to therapeutic agents. *J Clin Invest* 1999; **104:** 263–269.
518 27. Tamura T, Kuwahara A, Kadoyama K, *et al.* Effects of bolus injection of 5fluorouracil
519 on steady-state plasma concentrations of 5-fluorouracil in Japanese patients with
520 advanced colorectal cancer. *Int J Med Sci* 2011; **8:** 406–412.
521 28. Mouradov D, Sloggett C, Jorissen RN, *et al*. Colorectal cancer cell lines are
522 representative models of the main molecular subtypes of primary cancer. *Cancer Res*
523 2014; **74:** 3238–3247.
524 29. Herman SE, Gordon AL, Hertlein E, *et al*. Bruton tyrosine kinase represents a promising
525 therapeutic target for treatment of chronic lymphocytic leukemia and is effectively
526 targeted by PCI-32765. *Blood* 2011; **117:** 6287–6296.
527 30. MA J, Lu P, Guo A, *et al.* Characterization of ibrutinib-sensitive and -resistant mantle
528 lymphoma cells. *Br J Haematol* 2014; **166:** 849–861.
529 31. Cinar M, Hamedani F, Mo Z, *et al.* Bruton tyrosine kinase is commonly overexpressed
530 in mantle cell lymphoma and its attenuation by Ibrutinib induces apoptosis. *Leuk Res*
531 2013; **37:** 1271–1277.
532 32. Zheng X, Ding N, Song Y, *et al*. Different sensitivity of germinal center B cell-like diffuse
533 large B cell lymphoma cells towards ibrutinib treatment. *Cancer Cell Int* 2014; **14:** 32–
534 41.
535 33. Sun BB, Shah B, Fiskus W, *et al*. Synergistic activity of BET protein antagonistbased
536 combinations in mantle cell lymphoma cells sensitive or resistant to ibrutinib. *Blood*
537 2015; **126:** 1565–1574.

538 34. Grabinski N, Ewald F. Ibrutinib (ImbruvicaTM) potently inhibits ErbB receptor
539 phosphorylation and cell viability of ErbB2-positive breast cancer cells. *Invest New*
540 *Drugs* 2014; **32:** 1096–1104.
541 35. Gao W, Wang M, Wang L, *et al*. Selective antitumour activity of ibrutinib in EGFRmutant
542 non-small cell lung cancer cells. *J Natl Cancer Inst* 2014; **106:** pii: dju204.
543 36. Chen J, Kinoshita T, Sukbuntherng J, *et al*. Ibrutinib inhibits ERBB receptor tyrosine
544 kinases and HER2-amplified breast cancer cell growth. *Mol Cancer Ther* 2016; **15:**
545 2835–2844.
546 37. Chong CR, Jänne PA. The quest to overcome resistance to EGFR-targeted therapies
547 in cancer. *Nat Med* 2013; **19:** 1389–1400.
548 38. Müller, Bracken AP, Vernell R, *et al*. E2Fs regulate the expression of genes involved in
549 differentiation, development, proliferation, and apoptosis. *Genes Dev* 2001; **15:** 267–
550 285.
551 39. Helin K, Wu CL, Fattaey AR, *et al*. Heterodimerization of the transcription factors E2F-
552 1 and DP-1 leads to cooperative trans-activation. *Genes Dev* 1993; **7:** 1850– 1861.
553 40. Hitchens MR, Robbins PD. The role of the transcription factor DP in apoptosis.
554 *Apoptosis* 2003; **8:** 461–468.

555 41. Schweiger PJ and Jensen KB. Modeling human disease using organotypic cultures.
556 *Curr Opin Cell Biol* 2016; **43:** 22–29.
557 42. Vlachogiannis G, Hedayat S, Vatsiou A, *et al*. Patient-derived organoids model
558 treatment response of metastatic gastrointestinal cancers. *Science* 2018; 3**59:** 920–
559 926.
560 43. Ponader S, Chen SS, Buggy JJ, *et al*. The Bruton tyrosine kinase inhibitor PCI32765
561 thwarts chronic lymphocytic leukemia cell survival and tissue homing in vitro and in
562 vivo. *Blood* 2012; **107:** 1182–1189.

563 44. Basile D, Gerratana L, Buonadonna A *et al*. Role of Bruton's Tyrosine Kinase in Stage
564 III Colorectal Cancer. *Cancers (Basel)* 2019; **11:** pii: E880.
565 45. Yamaoka T, Ohba M and Ohmori T. Molecular-targeted therapies for epidermal growth
566 factor receptor and its resistance mechanisms. *Int J Mol Sci* 2017; **18:** pii: E2420.
567 46. Singh J, Petter RC, Kluge AF. Targeted covalent drugs of the kinase family. *Curr Opin*
568 *Chem Biol* 2010; **14:** 475–480.
569 47. Young WB, Barbosa J, Blomgren P, *et al*. Potent and selective Bruton's tyrosine kinase
570 inhibitors: discovery of GDC-0834. *Bioorg Med Chem Lett* 2015; **25:** 1333– 1337.
571 48. Lou Y, Han X, Kuglstatter A, *et al*. Structure-based drug design of RN486, a potent and
572 selective Bruton's tyrosine kinase (BTK) inhibitor, for the treatment of rheumatoid
573 arthritis. *J Med Chem* 2015; **58:** 512–516.
574 49. Middendorp S, Dingjan GM, Maas A, *et al*. Function of Bruton's tyrosine kinase during
575 B cell development is partially independent of its catalytic activity. *J Immunol* 2003; **171:**
576 5988–5996.
577 50. Romano G, Santi L, Bianco MR, *et al*. TGF-β pathway is activated by 5-fluorouracil
578 treatment in drug resistant colorectal carcinoma cells. *Oncotarget* 2016; **7:** 22077–
579 22091.
580 51. Kirshner J, Jobling MF, Pajares MJ, *et al*. Inhibition of transforming growth factorbeta1
581 signaling attenuates ataxia telangiectasia mutated activity in response to genotoxic
582 stress. *Cancer Res* 2006; **66:** 10861–10869
583 52. Lane DP. Cancer. p53, guardian of the genome. *Nature* 1992; **358:**15.
584 53. Polager S, Ginsberg D. p53 and E2F: partners in life and death. *Nat Rev Cancer* 2009;
585 **9:** 738.
586 54. Colak S, Medema JP. Cancer stem cells – important players in tumour therapy
587 resistance. *FEBS J* 2014; **281:** 4779–4791.

588 55. van de Wetering, M, Francies HE, Francis JM, *et al*. Prospective derivation of a living
589 organoid biobank of colorectal cancer patients. *Cell* 2015; **161:** 933–945.
590 56. Cantrell MA, Kuo CJ. Organoid modeling for cancer precision medicine. *Genome Med*
591 2015; **7:** 32.
592 57.Scheers E, Leclercq L, de Jong J, *et al*. Absorption, metabolism, and excretion of oral
593 ^{14}C radiolabeled ibrutinib: an open-label, phase I, single-dose study in healthy men.
594 *Drug Metab Dispos* 2015; **43:** 289–296.
595 58. Lolodi O, Wang Y-M, Wright WC, *et al*. Differential regulation of CYP3A4 and CYP3A5
596 and its implication in drug discovery. *Curr Drug Metab* 2017; **18:** 1095– 1105.
597 59. Hohmann N, Haefeli WE, Mikus G. CYP3A activity: towards dose adaptation to the
598 individual. *Expert Opin Drug Metab Toxicol* 2016; **12:** 479–497.
599 60. Finnes HD, Chaffee KG, Call TG, *et al*. Pharmacovigilance during ibrutinib therapy for
600 chronic lymphocytic leukemia (CLL)/small lymphocytic lymphoma (SLL) in routine
601 clinical practice. *Leuk Lymphoma* 2017; **58:** 1376–1383.
602 61. Koch I, Weil R, Wolbold R, *et al*. Interindividual variability and tissue-specificity in the
603 expression of cytochrome P450 3A mRNA. *Drug Metab Dispos* 2002; **30:** 1108– 1114.
604 62. Smith CI. From identification of the BTK kinase to effective management of leukemia.
605 *Oncogene* 2017; **36:** 2045–2053.
606 63. Brown JR, Harb WA, Hill BT, *et al*. Phase 1 study of single-agent CC-292, a highly
607 selective Bruton's tyrosine kinase inhibitor, in relapsed or refractory chronic lymphocytic
608 leukemia. *Haematologica* 2016; **101:** e295–298.
609 64. Walter HS, Rule SA, Dyer MJ, *et al*. A phase 1 clinical trial of the selective BTK inhibitor
610 ONO/GS-4059 in relapsed and refractory mature B-cell malignancies.
611 *Blood* 2016; **127:** 411–419.
612 65. Ghia. P. Ibrutinib holds promise for patients with 17p deletion CLL. *Lancet Oncol* 2016;
613 **17:** 1342–1343.

66. https://www.imbruvica.com/docs/librariesprovider7/default-documentlibrary/prescribing_information.pdf. Revised 01/2019.

67. Fransson A, Glaessgen D, Alfredsson J, *et al*. Strong synergy with APR-246 and DNA-damaging drugs in primary cancer cells from patients with TP53 mutant highgrade serous ovarian cancer. *J Ovarian Res* 2016; **9:** 27–36

*68. Sato T, Stange DE, Ferrante M. *et al*. Long-term expansion of epithelial organoids from human colon, adenoma, adenocarcinoma, and Barrett's epithelium. *Gastroenterology* 2011; **141:** 1762–1772.

*69. Weeber F, van de Wetering M, Hoogstraat M, *et al*. Preserved genetic diversity in organoids cultured from biopsies of human colorectal cancer metastases. *Proc Natl Acad Sci USA* 2015; **112:** 13308–13311.

*70. Holmberg C, Helin K, Sehested M, *et al*. E2F-1-induced p53-independent apoptosis in transgenic mice. Oncogene 1998; **17:** 143–155.

*Cited only in supplementary materials.

TABLES

	IBRUTINIB		**AVL-292**		**CGI1746**		**ONO-4059**		**RN486**	
	10μM	**20μM**	**10μM**	**20μM**	**10μM**	**20μM**	**10μM**	**20μM**	**10μM**	**20μM**
HCT116 p53KO	0.2	0.2	0.3	0.3	0.2	0.2	0.2	0.2	0.2	0.3

SW480	0.3	0.3	0.5	0.5	0.3	0.3	0.3	0.3	0.3	0.3
HT-29	0.4	0.4	0.4	0.4	0.3	0.4	0.4	0.14	0.4	0.4

Table 1. Synergism between BTK inhibitors and 5-FU in cell lines. Combination Index (CI) was calculated as reported by Fransson, *et al* [67] and detailed in Materials and methods.

0.8 < CI < 1.2 = additive effect

CI < 0.8 = synergistic effect (CI < 0.5 = strong synergistic effect) CI > 1.2 = sub-additive effect.

ant = antagonistic effect

	TUM01	**TUM03**	**TUM07**	**TUM09**	**ITO17**
5-FU+IBRU	0.3	0.2	0.2	0.01	1.1
5-FU+AVL	0.1	0.5	0.1	0.2	0.7

Table 2. Synergism between BTK inhibitors and 5-FU in organoids. Combination Index (CI) was calculated as reported by Fransson, *et al* [67] and detailed in Materials and methods.

0.8 < CI < 1.2 = additive effect

640 CI < 0.8 = synergistic effect (CI < 0.5 = strong synergistic effect) CI >

641 1.2 = sub-additive effect.

642 ant = antagonistic effect

643 **LEGENDS TO FIGURES**

644 **Figure 1**. p65BTK expression correlates with cancer progression. (A) Expression of

645 p65BTK quantified by ELISA using the BN33 antibody in two cohorts of CRC patients (*n*=90)

646 according to the Grade of the disease; PT: peri-tumour normal tissue; T: tumour tissue; G1,

647 G2, G3 tumour tissue grade 1, 2, 3 respectively. A two-tailed Student's *t*-test was used for

648 comparing p65BTK levels in PT versus T tissue. (B) p65BTK expression in colon cancer

649 stem cells (CSC) lysates and stem cell-enriched organoids from colon cancer patients

650 detected with BN49 antibody. β-Actin was used as a loading control. (C) Examples of

651 p65BTK expression in different histotypes of colon cancers and in normal colon detected

652 by BN30 antibody. Bar: 100 μm; 20X objective magnification. (D) IHC was performed using

653 BN30, and p65BTK staining was graded according to the percentage of positive cells in the

654 area. Examples of 0%, 30%, 70% and 100% positive samples. Bar = 100 μm; 20X objective

655 magnification. (E) Left: Percentage of p65BTKpositive samples from patients (any positivity)

656 at different stage of CRC. Right:

657 Percentage of p65BTK-expressing cells in samples from patients at different stage of CRC.

658 Stage I, *n*=43 Stage II, *n*=44 Stage III, *n*=87.

659 **Figure 2.** p65BTK levels determine 5-FU sensitivity of colon carcinoma cells. (A) *Left:*

660 p65BTK levels in drug-resistant HCT116p53KO cells stably infected with empty (pRS) or

661 shBTK-encoding (pRSBTK) vectors. *Right:* p65BTK fold-change evaluated by ImageJ

662 analysis of the blot shown in A. (B) Percentage cell death after 72 h treatment with 200 μM
663 5-FU of HCT116p53KO-pRS or HCT116p53KO-pRSBTK cells. Parental drug-
664 sensitive HCT116 cells were treated in parallel as a positive control. (C) *Left:* p65BTK levels
665 in HCT116p53KO cells not transfected (NT) or transiently transfected with control siRNA
666 (LUC) or siRNA for BTK**.** *Right*: p65BTK fold-change evaluated by ImageJ analysis of the
667 blot shown in C. (D) Percentage of cell death after 72 h treatment with 200 μM 5-FU of
668 HCT116p53KO-NT, HCT116p53KO-siLUC and HCT116p53KO-siBTK. (E) *Left:* p65BTK
669 levels in parental HCT116 cells transiently transfected with empty vector (empty) or a
670 p65BTK-encoding vector (HCT116p65BTK) or its kinase-dead (HCT116p65BTK-KD)
671 counterpart. HCT116p53KO lysate was loaded as a control. *Right*: p65BTK fold-change
672 evaluated by ImageJ analysis of the blot shown in E. In A,C,E p65BTK was detected by
673 BN49 antibody and β-Actin was used as a loading control. (F) Percentage cell death after
674 72 h treatment with 200 μM 5-FU of HCT116empty, HCT116-p65BTK and HCT116p65BTK-
675 KD cells. HCT116p53KO cells were treated in parallel as a control. (G) Percentage of cell
676 death after 72 h treatment of HCT116 cells with maximally effective concentrations of 5-FU
677 (200 μM), non-toxic concentrations of 5-FU (10 μM), ibrutinib (IBRU, 10 μM) and the
678 combination thereof. (H) Percentage cell death after 72 h treatment of HCT116p53KO cells
679 with 200 μM 5FU in the presence of increasing concentrations of ibrutinib (IBRU). In B, D,
680 F, G, H cell death was evaluated by Trypan blue exclusion. All graphs represent the average
681 of at least 3 independent experiments; bars show mean ± sem (n=3); a two-tailed Student's
682 *t*test was used for comparing 5-FU-treated versus untreated cells.

683 **Figure 3**. Inhibition of p65BTK abolishes 5-FU resistance of TP53-null colon carcinoma
684 cells**.** Percentage of cell death, as evaluated by Trypan blue exclusion, after 72 h treatment
685 of HCT116p53KO (A) SW480 (B) and HT-29 (C) cells with 200 μM 5-FU (FU) ± 10 or 20
686 μM of the different BTK inhibitors. AVL = AVL-292; CGI = CGI1746; ONO = ONO-4059; RN
687 = RN486. All graphs represent the average of at least 3 independent experiments; bars
688 show mean ± sem (n=3); a two-tailed Student's *t*-test was used for comparing combined
689 treatments to 5-FU alone.
690 **Figure 4.** p65BTK inhibition blunts protective 5-FU-elicited TGFB1-mediated transcription
691 and induces pro-apoptotic E2F activation. (A) Modulation of TGFB1mediated transcription
692 after treatment of HCT116p53KO cells with 200 μM 5-FU, 20 μM Ibrutinib (IBRU) or the
693 combination, as assessed by reporter assay. Results are plotted as fold-change, calculated
694 as the ratio: values of treated cells/values of untreated cells, and where the value of
695 untreated cells is set at 1. Bars show mean ± sem (n=3); a twotailed Student's *t*-test was
696 used for comparing combined versus single treatments. (B) Percentage cell death, as
697 evaluated by Trypan blue exclusion, in the absence of treatment (NT) or after 72 h treatment
698 of HCT116p53KO with 200 μM 5-FU, a combination of 200 μM 5-FU + 20 μM Ibrutinib (5-
699 FU+IBRU), the same combination in conditioned medium harvested from drug-resistant
700 HCT116p53KO cells treated for 6 h with 200 μM 5-FU, in absence (FU+IBRU+CM) or in
701 presence of 20 μM TGFB1R inhibitor SB431542 (FU+IBRU+CM+TGFB1R). (C) Modulation
702 of E2F-mediated transcription after treatment of HCT116p53KO cells with 200 μM 5-FU, 20

μM Ibrutinib (IBRU) or the combination, as assessed by reporter assay. Results are plotted as foldinduction and statistics (*n=3*) is performed as in A. (D) Percentage cell death, as evaluated by Trypan blue exclusion, after 72 h in absence of treatment (NT) and upon treatment with 200 μM 5-FU and the combination 200 μM 5-FU + 20 μM Ibrutinib (5FU+IBRU) of HCT116p53KO transfected with control (LUC) or TFDP1-targeted siRNA. (E) Percentage cell death, as evaluated by Trypan blue exclusion, in absence of treatment (NT) or after 72 h treatment with 200 μM 5-FU, 200 μM 5-FU + 20 μM Ibrutinib (5-FU+IBRU), 5-FU + Ibrutinib + 10ng/ml TGFB1 (5-FU+IBRU+TGFB1) of HCT116p53KO transfected with control (LUC) or DP1-targeted siRNA. In the insets in D and E: TFDP1 expression in Luc- versus TFDP1-silenced HCT116p53KO cells. B, D, E: bars show mean ± sem (n=3). *n* = 3. A two-tailed Student's *t*-test was used for comparing the different treatments.

Figure 5. *Ex vivo* p65BTK inhibition sensitizes p53-null colon cancer stem cell-enriched organoids to 5-FU. Percentage cell survival after 72 h treatment with 100 μM 5-FU alone or in combination with non-toxic doses of ibrutinib (IBRU) or AVL-292 (AVL) (as determined by the dose-response curves, see supplementary material, Figure S9). Cell viability was evaluated by Cell-Titer Glo before adding the treatments (T_0) and 72 h later. T_0 values correspond to 100% viability; 72 h values are then expressed as the percentage variation relative to the initial cell number. TUM01: IBRU 30μM, AVL 10 μM; TUM03: IBRU 30μM, AVL 20μM; TUM07: IBRU 20μM, AVL 30μM; TUM09: IBRU 10μM, AVL 2μM; ITO17: IBRU 30μM, AVL 20μM. Bars show mean ± sem (n=3). A two-tailed Student's *t*-test was used for comparing combined treatments to 5-FU alone.

Figure 6. *In vivo* p65BTK inhibition sensitizes drug-resistant p53-null colon carcinomas to 5-FU**. (**A) kinetics of growth of HCT116p53KO xenografts after treatment with vehicle alone

(CNT), 5-FU 60 mg/kg (FU), ibrutinib 25 mg/kg (IBRU 25), ibrutinib 25 mg/kg + 5FU 60 mg/kg (IBRU 25+FU). (B) Range of relative tumour volumes (RTV) of HCT116p53KO xenografts measured at the end of the treatment (21 days) of mice with vehicle alone (CNT), 5-FU 60 mg/kg (FU), ibrutinib 25 mg/kg (IBRU 25), ibrutinib 25 mg/kg + 5-FU 60 mg/kg (IBRU 25+FU). (C) Tumour duplication (TDT) time of HCT116p53KO xenografts calculated at the end of the treatment (21 days) of mice with vehicle alone (CNT), 5-FU 60 mg/kg (FU), ibrutinib 25 mg/kg (IBRU 25), ibrutinib 25 mg/kg + 5-FU 60 mg/kg (IBRU 25+FU). TDT was calculated by the formula TDT=DXD0*log10(2)/(log10VX- log10V0), where DX-D0= days of treatment, VX=volume at day X, V0= volume at day 0 (start of the treatment). The bold line indicates the median of the values, the box indicates the first and third quartile. The maximum and minimum values for each group are also reported. (D) Model of cancer cell fate decisions following p65BTK inhibition. In TP53-null colon cancers expressing high levels of p65BTK 5-FU treatment induces a TGFB1-mediated anti-apoptotic response. Reducing p65BTK expression or inhibiting it pharmacologically when administering 5-FU abolishes the TGFB1 protective response and triggers E2F-dependent apoptosis.

SUPPLEMENTARY MATERIAL ONLINE

Supplementary materials and methods

Figure S1. Characterization of Anti-p65BTK antibodies

Figure S2. p65BTK expression levels are post-transcriptionally regulated downstream of the RAS/MAPK pathway

Figure S3. The synergic effect of ibrutinib and 5-FU is stronger in TP53-null/RASmutated versus TP53-null/RAS-wild type colon cancer cells

Figure S4. Sensitizing action of ibrutinib is not due to cross-inhibition of EGFR family members

Figure S5. p65BTK inhibition restores the apoptotic response of drug-resistant TP53null colon cells to 5-FU

Figure S6. Changes in transcriptional activity following p65BTK inhibition in presence of 5-FU

Figure S7. Blocking 5-FU-induced TGFB1 downregulates its targets and attenuates drug resistance

Figure S8. E2F targets are up-regulated following 5-FU treatment in presence of BTK inhibition

Figure S9. Molecular characterization and dose-response curves of organoids treated with 5-FU or BTK inhibitors

Figure S10. In vivo p65BTK inhibition does not ameliorate the response of drugsensitive HCT116 xenografts to 5FU

Table S1. Known genetic alterations characterizing the different colon carcinoma cell lines used in the paper

Figure 1

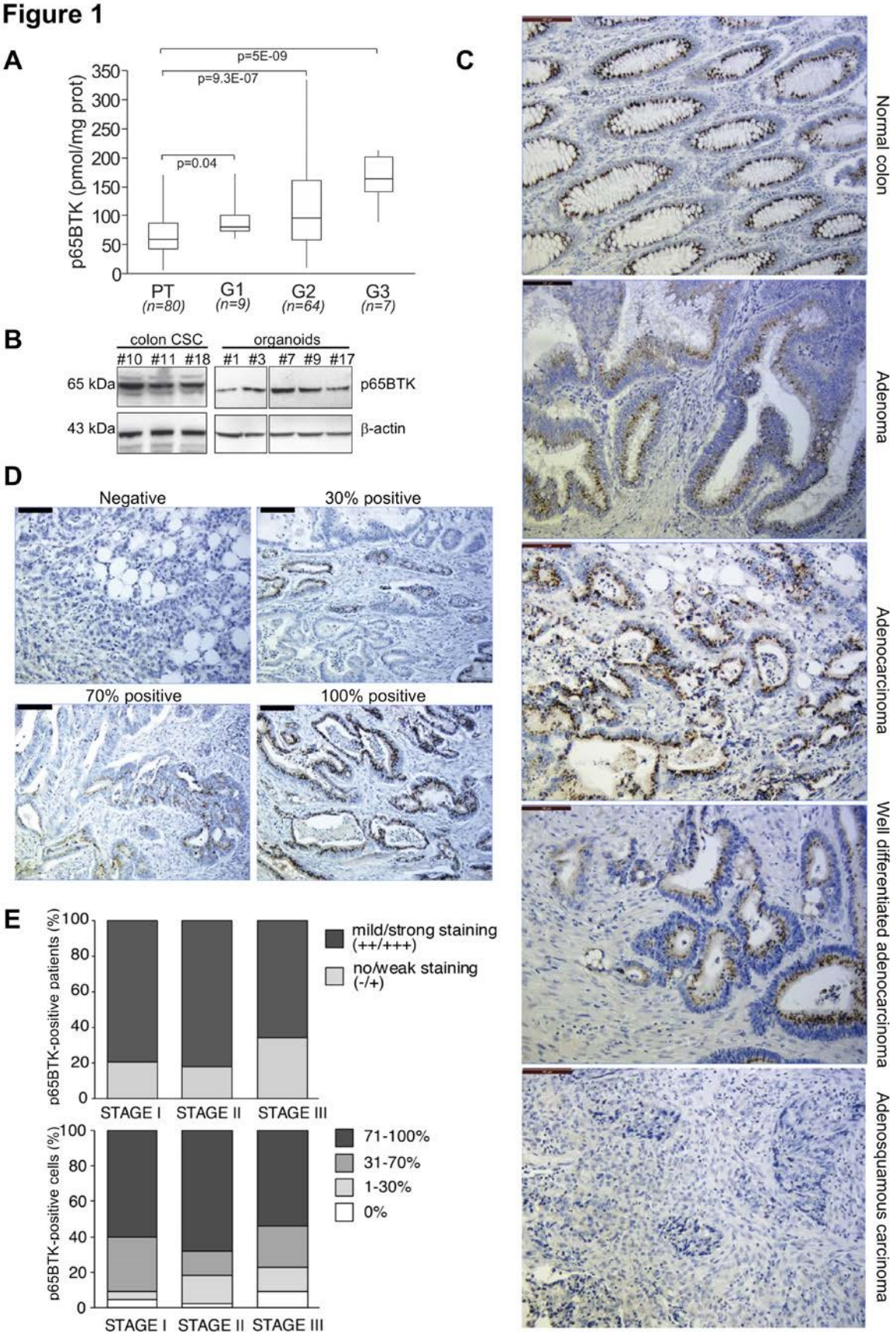
A
p=5E-09
p=9.3E-07
p=0.04
p65BTK (pmol/mg prot)
350
300
250
200
150
100
50
0
PT (n=80)
G1 (n=9)
G2 (n=64)
G3 (n=7)
B
colon CSC
organoids
#10 #11 #18
#1 #3 #7 #9 #17
65 kDa
p65BTK
43 kDa
β-actin
C
Normal colon
Adenoma
Adenocarcinoma
Well differentiated adenocarcinoma
Adenosquamous carcinoma
D
Negative
30% positive
70% positive
100% positive
E
p65BTK-positive patients (%)
mild/strong staining (++/+++)
no/weak staining (-/+)
STAGE I
STAGE II
STAGE III
p65BTK-positive cells (%)
71-100%
31-70%
1-30%
0%

Figure 2

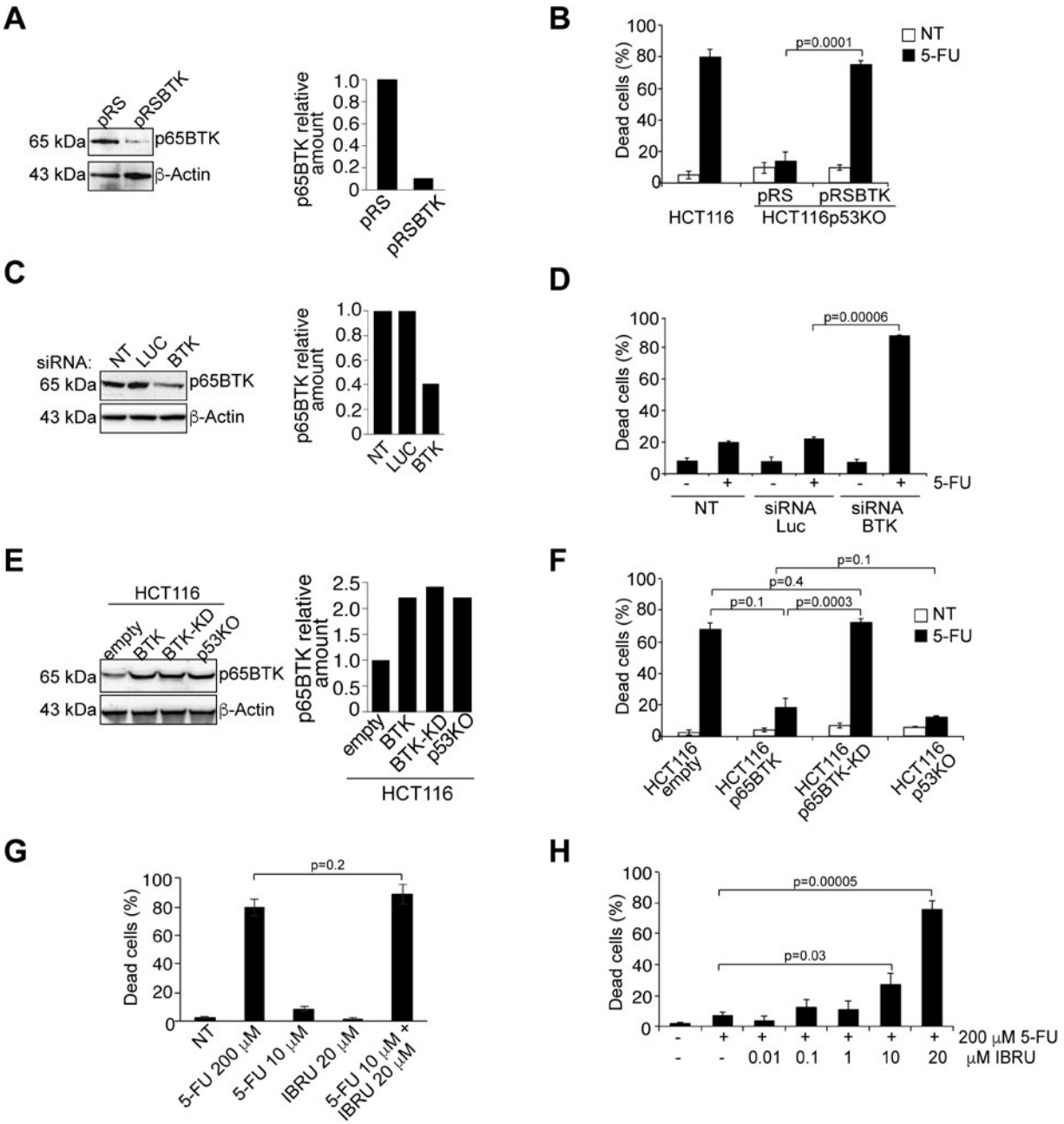

766

767

Figure 3

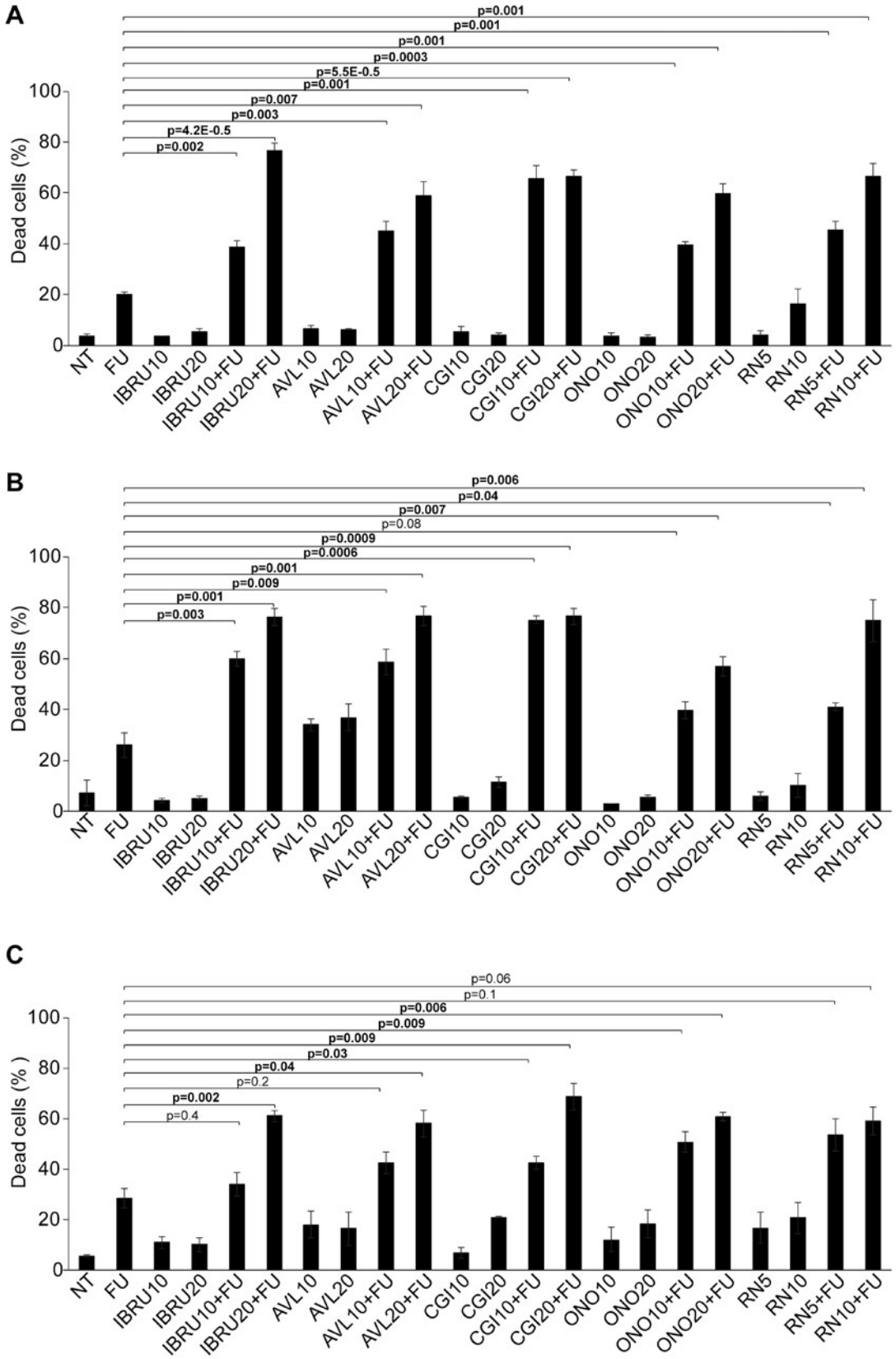
A
p=0.001
p=0.001
p=0.001
p=0.0003
p=5.5E-0.5
p=0.001
p=0.007
p=0.003
p=4.2E-0.5
p=0.002
Dead cells (%)
100
80
60
40
20
0
NT
FU
IBRU10
IBRU20
IBRU10+FU
IBRU20+FU
AVL10
AVL20
AVL10+FU
AVL20+FU
CGI10
CGI20
CGI10+FU
CGI20+FU
ONO10
ONO20
ONO10+FU
ONO20+FU
RN5
RN10
RN5+FU
RN10+FU
B
p=0.006
p=0.04
p=0.007
p=0.08
p=0.0009
p=0.0006
p=0.001
p=0.009
p=0.001
p=0.003
Dead cells (%)
100
80
60
40
20
0
NT
FU
IBRU10
IBRU20
IBRU10+FU
IBRU20+FU
AVL10
AVL20
AVL10+FU
AVL20+FU
CGI10
CGI20
CGI10+FU
CGI20+FU
ONO10
ONO20
ONO10+FU
ONO20+FU
RN5
RN10
RN5+FU
RN10+FU
C
p=0.06
p=0.1
p=0.006
p=0.009
p=0.009
p=0.03
p=0.04
p=0.2
p=0.002
p=0.4
Dead cells (%)
100
80
60
40
20
0
NT
FU
IBRU10
IBRU20
IBRU10+FU
IBRU20+FU
AVL10
AVL20
AVL10+FU
AVL20+FU
CGI10
CGI20
CGI10+FU
CGI20+FU
ONO10
ONO20
ONO10+FU
ONO20+FU
RN5
RN10
RN5+FU
RN10+FU

Figure 4

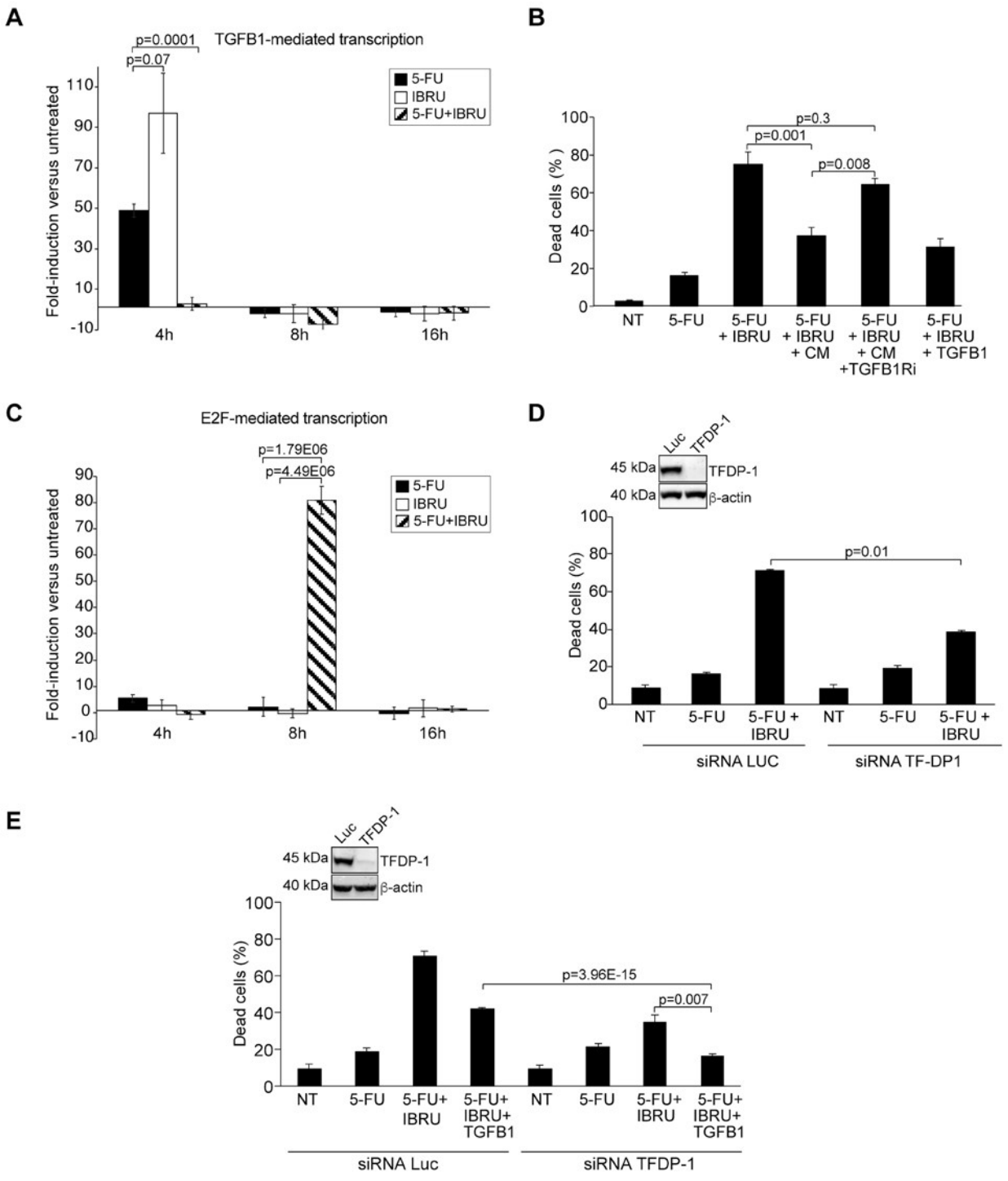
A
TGFB1-mediated transcription
p=0.0001
p=0.07
5-FU
IBRU
5-FU+IBRU
Fold-induction versus untreated
4h
8h
16h
B
p=0.3
p=0.001
p=0.008
Dead cells (%)
NT
5-FU
5-FU + IBRU
5-FU + IBRU + CM
5-FU + IBRU + CM +TGFB1Ri
5-FU + IBRU + TGFB1
C
E2F-mediated transcription
p=1.79E06
p=4.49E06
D
Luc
TFDP-1
45 kDa
40 kDa
β-actin
p=0.01
Dead cells (%)
siRNA LUC
siRNA TF-DP1
E
p=3.96E-15
p=0.007
siRNA Luc
siRNA TFDP-1

Figure 5

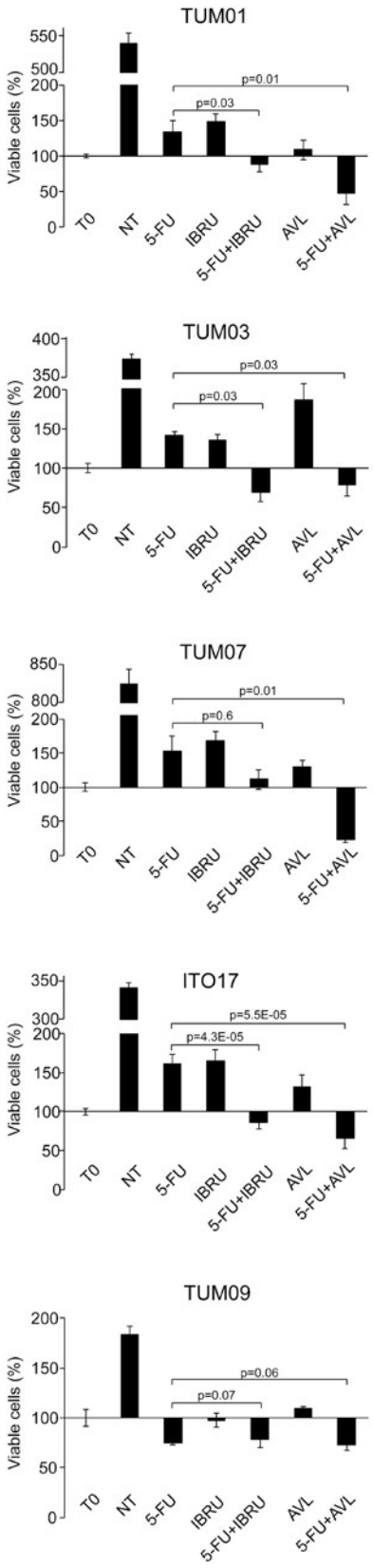
TUM01
Viable cells (%)
550
500
200
150
100
50
0
p=0.01
p=0.03
T0
NT
5-FU
IBRU
5-FU+IBRU
AVL
5-FU+AVL
TUM03
Viable cells (%)
400
350
200
150
100
50
0
p=0.03
p=0.03
T0
NT
5-FU
IBRU
5-FU+IBRU
AVL
5-FU+AVL
TUM07
Viable cells (%)
850
800
200
150
100
50
0
p=0.01
p=0.6
T0
NT
5-FU
IBRU
5-FU+IBRU
AVL
5-FU+AVL
ITO17
Viable cells (%)
350
300
200
150
100
50
0
p=5.5E-05
p=4.3E-05
T0
NT
5-FU
IBRU
5-FU+IBRU
AVL
5-FU+AVL
TUM09
Viable cells (%)
200
150
100
50
0
p=0.06
p=0.07
T0
NT
5-FU
IBRU
5-FU+IBRU
AVL
5-FU+AVL

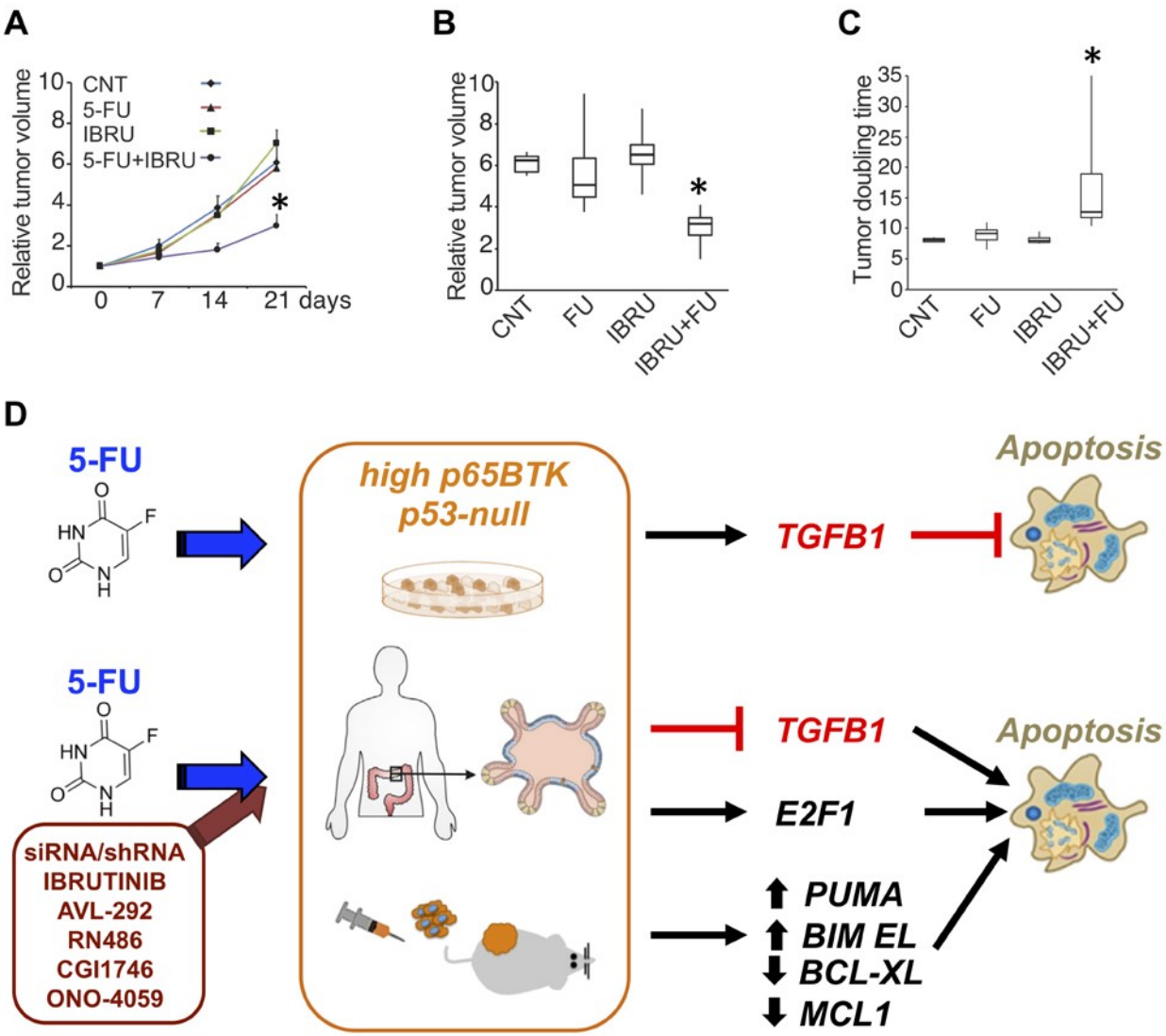
A
Relative tumor volume
CNT
5-FU
IBRU
5-FU+IBRU
0 7 14 21 days
B
Relative tumor volume
CNT FU IBRU IBRU+FU
C
Tumor doubling time
CNT FU IBRU IBRU+FU
D
5-FU
5-FU
siRNA/shRNA
IBRUTINIB
AVL-292
RN486
CGI1746
ONO-4059
high p65BTK
p53-null
TGFB1
Apoptosis
TGFB1
E2F1
Apoptosis
PUMA
BIM EL
BCL-XL
MCL1

774